

Higgs Physics

Abdelhak Djouadi*

Laboratoire de Physique Théorique, CNRS & Université Paris-Sud, 91405 Orsay, France

E-mail: abdelhak.djouadi@th.u-psud.fr

The implications of the discovery of a scalar Higgs boson at the LHC with a mass of approximately 125 GeV are summarised in the context of the Standard Model of particle physics with its unique scalar boson and of its most celebrated new physics extension, the minimal supersymmetric Standard Model or MSSM, in which the Higgs sector is extended to contain three neutral and two charged scalar bosons. Discussed are the implications from the measured mass, the production and decay rates of the observed particle and, in the MSSM, from the constraints in the search for the heavier Higgs states. The perspectives for Higgs and new physics searches at the next LHC upgrades as well as at future hadron and lepton colliders are then briefly summarized.

Proceedings of the Corfu Summer Institute 2014 "School and Workshops on Elementary Particle Physics and Gravity",

3-21 September 2014

Corfu, Greece

*Speaker.

1. Introduction

The ATLAS and CMS historical discovery of a particle with a mass of 125 GeV [1] and properties that are compatible with those of a scalar Higgs boson [2, 3] has far reaching consequences not only for the Standard Model (SM) but also for new physics models beyond it. In the SM, electroweak symmetry breaking is achieved spontaneously via the Brout–Englert–Higgs mechanism [2], wherein the neutral component of an isodoublet scalar field acquires a non-zero vacuum expectation value v . This gives rise to nonzero masses for the fermions and the electroweak gauge bosons while preserving the $SU(2) \times U(1)$ gauge symmetry. One of the four degrees of freedom of the original isodoublet field, corresponds to a physical particle [3]: a scalar boson with $J^{PC} = 0^{++}$ quantum numbers under parity and charge conjugation. The couplings of the Higgs boson to the fermions and gauge bosons are related to the masses of these particles and are thus decided by the symmetry breaking mechanism. In contrast, the mass of the Higgs boson itself M_H , although expected to be in the vicinity of the weak scale $v \approx 250$ GeV, is undetermined. Let us summarise the known information on this parameter before the start of the LHC.

A direct information was the lower limit $M_H \gtrsim 114$ GeV at 95% confidence level (CL) established at LEP2 [4]. Furthermore, a global fit of the electroweak precision data to which the Higgs boson contributes, yields the value $M_H = 92_{-26}^{+34}$ GeV, corresponding to a 95% CL upper limit of $M_H \lesssim 160$ GeV [4]. From the theoretical side, the presence of this new weakly coupled degree of freedom is a crucial ingredient for a unitary electroweak theory. Indeed, the SM without the Higgs particle leads to scattering amplitudes of the W/Z bosons that grow with the square of the center of mass energy and perturbative unitarity would be lost at energies above the TeV scale. In fact, even in the presence of a Higgs boson, the W/Z bosons could interact very strongly with each other and, imposing the unitarity requirement in the high-energy scattering amplitudes leads to the important mass bound $M_H \lesssim 700$ GeV [5], implying that the particle is kinematically accessible at the LHC.

Another theoretical constraint emerges from the fact that the Higgs self-coupling, $\lambda \propto M_H^2$, evolves with energy and at some stage, becomes very large and even infinite and the theory completely loses its predictability. If the energy scale up to which the couplings remains finite is of the order of M_H itself, one should have $M_H \lesssim 650$ GeV [6]. On the other hand, for small values of λ and hence M_H , the quantum corrections tend to drive the self-coupling to negative values and completely destabilize the scalar Higgs potential to the point where the minimum is not stable anymore [6]. Requiring $\lambda \geq 0$, up to the TeV scale implies that $M_H \gtrsim 70$ GeV. If the SM is to be extended to the Planck scale $M_P \sim 10^{18}$ GeV, the requirements on λ from finiteness and positivity constrain the Higgs mass to lie in the range $130 \text{ GeV} \lesssim M_H \lesssim 180 \text{ GeV}$ [6]. This narrow margin is close to the one obtained from the direct and indirect experimental constraints.

The discovery of the Higgs particle with a mass of 125 GeV, a value that makes the SM perturbative, unitary and extrapolable to the highest possible scales, is therefore a consecration of the model and crowns its past success in describing all experimental data available. In particular, the average mass value measured by the ATLAS and CMS teams, $M_H = 125.1 \pm 0.24$ GeV [7], is remarkably close to the best-fit of the precision data which should be considered as a great achievement and a triumph for the SM. In addition, a recent analysis that includes the state-of-the-art quantum corrections [8] gives for the condition of absolute stability of the electroweak vacuum, $\lambda(M_P) \geq 0$, the bound $M_H \gtrsim 129$ GeV for the present value of the top quark mass and the strong

coupling constant, $m_t^{\text{exp}} = 173.2 \pm 0.9$ GeV and $\alpha_s(M_Z) = 0.1184 \pm 0.0007$ [4]. Allowing for a 2σ variation of m_t^{exp} , one obtains $M_H \geq 125.6$ GeV that is close to the measured M_H value [7]. In fact, for an unambiguous and well-defined determination of the top mass, one should rather use the total cross section for top pair production at hadron colliders which can unambiguously be defined theoretically; this mass has a larger uncertainty, $\Delta m_t \approx 3$ GeV, which allows more easily for the absolute stability of the SM vacuum up to M_P ; see Ref. [9] for discussions on this issue.

Nevertheless, the SM is far from being perfect in many respects. It does not explain the proliferation of fermions and the large hierarchy in their mass spectra and does not say much about the small neutrino masses. The SM does not unify in a satisfactory way the electromagnetic, weak and strong forces, as one has three different symmetry groups with three coupling constants which shortly fail to meet at a common value during their evolution with the energy scale; it also ignores the fourth force, gravitation. Furthermore, it does not contain a particle that could account for the cosmological dark matter and fails to explain the baryon asymmetry in the Universe.

However, the main problem that calls for beyond the SM is related to the special status of the Higgs boson which, contrary to fermions and gauge bosons has a mass that cannot be protected against quantum corrections. Indeed, these are quadratic in the new physics scale which serves as a cut-off and hence, tend to drive M_H to very large values, ultimately to M_P , while we need $M_H = \mathcal{O}(100 \text{ GeV})$. Thus, the SM cannot be extrapolated beyond $\mathcal{O}(1 \text{ TeV})$ where new physics should emerge. This is the reason why we expect something new to manifest itself at the LHC.

There are three avenues for the many possibilities for this new physics beyond the SM [10]. There are first theories with extra space-time dimensions that emerge at the TeV scale (the cut-off is then not very high) and, second, composite models inspired from the strong interactions also at the TeV scale (and thus the Higgs is not a fundamental spin-zero particle). Some versions of these scenarios do not incorporate any Higgs particle in their spectrum and are thus ruled out by the Higgs discovery. However, the option that emerges in the most natural way is Supersymmetry (SUSY) [11] as it solves most of the SM problems discussed above. In particular, SUSY protects M_H as the quadratically divergent radiative corrections from standard particles are exactly compensated by the contributions of their supersymmetric partners. These sparticles should not be much heavier than 1 TeV not to spoil this compensation [12] and they should be thus produced at the LHC.

The Higgs discovery is very important for SUSY and, in particular, for its simplest low energy manifestation, the minimal supersymmetric Standard Model (MSSM) that indeed predicts a light Higgs state. In the MSSM, two Higgs doublet fields H_u and H_d are required, leading to an extended Higgs consisting of five Higgs bosons, two CP-even h and H , a CP-odd A and two charged H^\pm states [13]. Nevertheless, only two parameters are needed to describe the Higgs sector at tree-level: one Higgs mass, which is generally taken to be that of the pseudoscalar A boson M_A , and the ratio of vacuum expectation values of the two Higgs fields, $\tan\beta = v_d/v_u$, expected to lie in the range $1 \lesssim \tan\beta \lesssim 60$. The masses of the CP-even h, H and the charged H^\pm states, as well as the mixing angle α in the CP-even sector are uniquely defined in terms of these two inputs at tree-level, but this nice property is spoiled at higher orders [14]. For $M_A \gg M_Z$, one is in the so-called decoupling regime in which the h state is light and has almost exactly the SM-Higgs couplings, while the other CP-even H and the charged H^\pm bosons become heavy, $M_H \approx M_{H^\pm} \approx M_A$, and decouple from the massive gauge bosons. In this regime, the MSSM Higgs sector thus looks almost exactly as the one of the SM with its unique Higgs boson.

Nevertheless, contrary to the SM Higgs boson, the lightest MSSM CP–even h mass is bounded from above and, depending on the SUSY parameters that enter the important quantum corrections, is restricted to $M_h^{\max} \lesssim 130$ GeV [14] if one assumes a SUSY breaking scale that is not too high, $M_S \lesssim \mathcal{O}(1)$ TeV, in order to avoid too much fine-tuning in the model. Hence, the requirement that the MSSM h boson coincides with the one observed at the LHC, i.e. with $M_h \approx 125$ GeV and almost SM–like couplings as the LHC data seem to indicate, would place very strong constraints on the MSSM parameters, in particular the SUSY–breaking scale M_S . This comes in addition to the limits obtained from the search of the heavier Higgs states and the superparticles at the LHC.

In this lecture, the implications of the discovery of the Higgs boson at the LHC and the measurement of its couplings to other particles will be summarised and the prospects for future searches of new physics, in particular in the SUSY context, will be summarized.

2. Implications for the Standard Model

In many respects, the Higgs particle was born under a very lucky star as the mass value of ≈ 125 GeV allows to produce it at the LHC in many redundant channels and to detect it in a variety of decay modes. This allows detailed studies of the Higgs properties as will be discussed here.

2.1 Higgs production and decay

We start by summarizing the production and decay at the LHC of a light SM–like Higgs particle, which should correspond to the lightest MSSM h boson in the decoupling regime. First, for $M_H \approx 125$ GeV, the Higgs mainly decays into $b\bar{b}$ pairs but the decays into WW^* and ZZ^* final states, before allowing the gauge bosons to decay leptonically $W \rightarrow \ell\nu$ and $Z \rightarrow \ell\ell$ ($\ell = e, \mu$), are also significant. The $H \rightarrow \tau^+\tau^-$ channel (as well as the gg and $c\bar{c}$ decays that are not detectable at the LHC) is also of significance, while the clean loop induced $H \rightarrow \gamma\gamma$ mode can be easily detected albeit its small rates. The very rare $H \rightarrow Z\gamma$ and even $H \rightarrow \mu^+\mu^-$ channels should be accessible at the LHC but only with a much larger data sample. This is illustrated in Fig. 1 (left) where the Higgs decay branching fractions are displayed for the narrow mass range $M_H = 120$ – 130 GeV [15].

On the other hand, many Higgs production processes have significant cross sections [18, 19] as is shown in the right–hand side of Fig. 1 where they are displayed at a proton collider at various past, present and foreseen center of mass energies for a 125 GeV SM–like Higgs boson. While the by far dominant gluon fusion mechanism $gg \rightarrow H$ (ggF) has extremely large rates (≈ 20 pb at $\sqrt{s} = 7$ – 8 TeV), the subleading channels, i.e. the vector boson fusion (VBF) $qq \rightarrow V^*V^* \rightarrow Hqq$ and the Higgs–strahlung (HV) $q\bar{q} \rightarrow HV$ with $V = W, Z$ mechanisms, have cross sections which should allow for a study of the Higgs particle already at $\sqrt{s} \gtrsim 7$ TeV with the amount of integrated luminosity, ≈ 25 fb $^{-1}$, that has been collected by each experiment. The Higgs–top associated process $pp \rightarrow t\bar{t}H$ (ttH) would require higher energy and luminosity.

This pattern already allows ATLAS and CMS to observe the Higgs boson in several channels and to measure some of its couplings in a reasonably accurate way. The channels that have been searched are $H \rightarrow ZZ^* \rightarrow 4\ell^\pm$, $H \rightarrow WW^* \rightarrow 2\ell 2\nu$, $H \rightarrow \gamma\gamma$ where the Higgs is mainly produced in ggF with subleading contributions from Hjj in the VBF process, $H \rightarrow \tau\tau$ where the Higgs is produced in association with one (in ggF) and two (in VBF) jets, and finally $H \rightarrow b\bar{b}$ with the Higgs produced in the HV process. One can ignore for the moment the additional search channels $H \rightarrow \mu\mu$ and $H \rightarrow Z\gamma$ for which the sensitivity is still too low with the data collected so far.

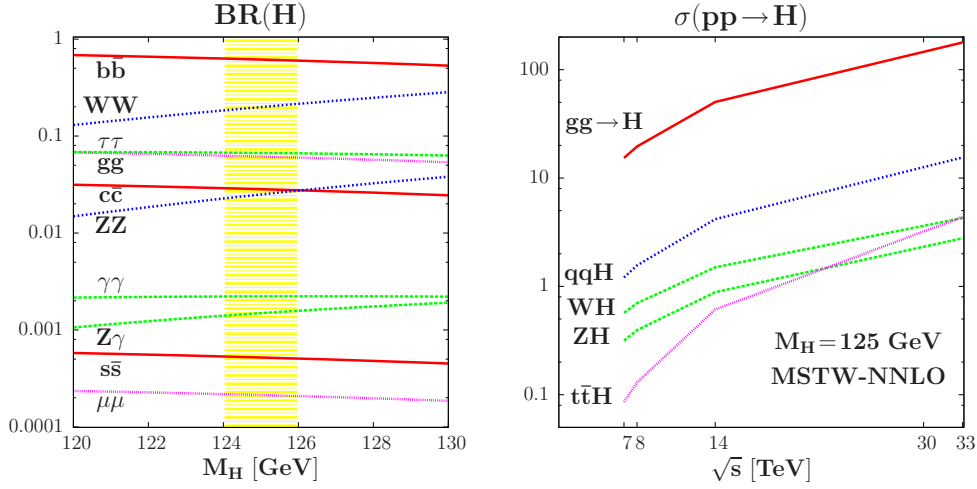


Figure 1: The SM-like Higgs boson branching ratios in the mass range 120–130 GeV (left) and its production cross sections at proton colliders as a function of the c.m. energy (right); from Ref. [20].

A convenient way to scrutinize the couplings of the produced H boson is to look at their deviation from the SM expectation. One then considers for a given search channel the signal strength modifier μ which for the $H \rightarrow XX$ decay mode measures the deviation compared to the SM expectation of the Higgs production cross section times decay branching fraction

$$\mu_{XX}|_{\text{th}} = \frac{\sigma(pp \rightarrow H \rightarrow XX)}{\sigma(pp \rightarrow H \rightarrow XX)|_{\text{SM}}} = \frac{\sigma(pp \rightarrow H) \times \text{BR}(H \rightarrow XX)}{\sigma(pp \rightarrow H)|_{\text{SM}} \times \text{BR}(H \rightarrow XX)|_{\text{SM}}}. \quad (2.1)$$

ATLAS and CMS have provided the signal strengths for the various final states with a luminosity of $\approx 5 \text{ fb}^{-1}$ for the 2011 run at $\sqrt{s} = 7 \text{ TeV}$ and $\approx 20 \text{ fb}^{-1}$ for the 2012 run at $\sqrt{s} = 8 \text{ TeV}$. The constraints given by the two collaborations are shown in Fig. 2. When combined, this leads to a global signal strength [7]:

$$\mu_{\text{tot}}^{\text{ATLAS}} = 1.18 \pm 0.15, \quad \mu_{\text{tot}}^{\text{CMS}} = 1.00 \pm 0.14 \quad (2.2)$$

The global signal strength being very close to unity, it implies that the observed Higgs is SM-like.

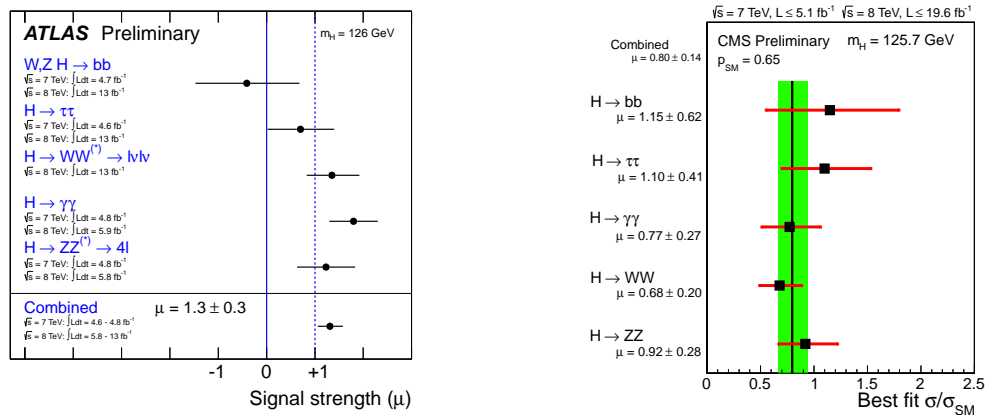


Figure 2: The signal strengths on the SM Higgs boson in the various search channels provided by ATLAS and CMS with the data collected so far at $\sqrt{s} = 7+8 \text{ TeV}$; from the summary given in Ref. [7].

2.2 The theoretical uncertainties and the signal strength ratios

As can be seen, already with the rather limited statistics at hand, the accuracy of the ATLAS and CMS measurements in eq. (2.2) is reaching the 15% level. This is at the same time impressive and worrisome. Indeed, the main Higgs production channel is the top and bottom quark loop mediated gluon fusion mechanism and, at $\sqrt{s}=7$ or 8 TeV, the three other mechanisms contribute at a total level below 15%. The majority of the signal events observed at LHC, in particular in the search channels $H \rightarrow \gamma\gamma, H \rightarrow ZZ^* \rightarrow 4\ell, H \rightarrow WW^* \rightarrow 2\ell 2\nu$ and, to a lesser extent $H \rightarrow \tau\tau$, thus come from the ggF mechanism which is known to be affected by large theoretical uncertainties.

Indeed, although $\sigma(gg \rightarrow H)$ is known up next-to-next-to-leading order (NNLO) in perturbative QCD (and at least at NLO for the electroweak interaction) [16–19], there is a significant residual scale dependence which points to the possibility that still higher order contributions cannot be totally excluded. In addition, as the process is of $\mathcal{O}(\alpha_s^2)$ at LO and is initiated by gluons, there are sizable uncertainties due to the gluon parton distribution function (PDF) and the value of the coupling α_s . A third source of theoretical uncertainties, the use of an effective field theory (EFT) approach to calculate the radiative corrections beyond the NLO approximation, should in principle also be considered [18]. In addition, large uncertainties arise when the $gg \rightarrow H$ cross section is broken into the jet categories $H+0j, H+1j$ and $H+2j$ [21]. In total, the combined theoretical uncertainty is estimated to be $\Delta^{\text{th}} \approx \pm 15\%$ [19] and would increase to $\Delta^{\text{th}} \approx \pm 20\%$ if the EFT uncertainty is also included. The a priori cleaner VBF process will be contaminated by the $gg \rightarrow H+2j$ mode making the total uncertainty in the $H+jj$ ‘‘VBF’’ sample also rather large [21].

Hence, the theoretical uncertainty is already at the level of the accuracy of the cross section measured by the ATLAS and CMS collaborations, eq. (2.2). Another drawback of the analyses is that they involve strong theoretical assumptions on the total Higgs width since some contributing decay channels not accessible at the LHC are assumed to be SM-like and possible invisible Higgs decays in scenarios beyond the SM are supposed not to occur. In Ref. [20], following earlier work [22], it has been suggested to consider the decay ratios D_{XX} defined as

$$D_{XX}^p = \frac{\sigma^p(pp \rightarrow H \rightarrow XX)}{\sigma^p(pp \rightarrow H \rightarrow VV)} = \frac{\sigma^p(pp \rightarrow H) \times \text{BR}(H \rightarrow XX)}{\sigma^p(pp \rightarrow H) \times \text{BR}(H \rightarrow VV)} = \frac{\Gamma(H \rightarrow XX)}{\Gamma(H \rightarrow VV)} \propto \frac{c_X^2}{c_V^2} \quad (2.3)$$

for a specific production process p and for a given decay channel $H \rightarrow XX$ when the reference channel $H \rightarrow VV$ is used. In these ratios, the cross sections $\sigma^p(pp \rightarrow H)$ and hence, their significant theoretical uncertainties will cancel out, leaving out only the ratio of partial decay widths which are affected by much smaller uncertainties. The total decay width which includes contributions from channels not under control such as possible invisible Higgs decays, do not appear in the ratios D_{XX}^p . Some common experimental systematical uncertainties such as the one from the luminosity measurement and the small uncertainties in the Higgs decay branching ratios also cancel out. We are thus left with only with the statistical and some (non common) systematical errors [20].

The ratios D_{XX} involve, up to kinematical factors and known radiative corrections, only the ratios $|c_X|^2/|c_V|^2$ of the Higgs reduced couplings to the particles X and V compared to the SM expectation, $c_X \equiv g_{HXX}/g_{HXX}^{\text{SM}}$. For the time being, three independent ratios can be considered: $D_{\gamma\gamma}, D_{\tau\tau}$ and D_{bb} . In order to determine these ratios, the theoretical uncertainties have to be treated as a bias (and not as if they were associated with a statistical distribution) and the fit should be performed for the two μ extremal values: $\mu_i|_{\text{exp}} \pm \delta\mu_i/\mu_i|_{\text{th}}$ with $\delta\mu_i/\mu_i|_{\text{th}} \approx \pm 20\%$ [23].

A large number of analyses of the Higgs couplings from the LHC data have been performed and in most cases, it is assumed that the couplings of the Higgs boson to the massive W, Z gauge bosons are equal, $g_{HZZ} = g_{HWW} = c_V$, and the couplings to all fermions are also the same $g_{Hff} = c_f$. However, as for instance advocated in Ref. [24] to characterize the Higgs particle at the LHC, at least three independent H couplings should be considered, namely c_t , c_b and c_V . One can thus define the following effective Lagrangian (in which the custodial symmetry relation $c_W = c_Z$ which holds in most cases is assumed) for the Higgs interactions

$$\mathcal{L}_H = c_V g_{HVV} H V_\mu V^\mu + c_t y_t H \bar{t}_L t_R - c_t y_c H \bar{c}_L c_R - c_b y_b H \bar{b}_L b_R - c_b y_\tau H \bar{\tau}_L \tau_R + \text{h.c.} \quad (2.4)$$

where $y_{t,c,b,\tau} = m_{t,c,b,\tau}/v$ are the Yukawa couplings of the heavy SM fermions, $g_{HWW} = 2M_W^2/v$ and $g_{HZZ} = M_Z^2/v$ the HWW and HZZ couplings and v the SM Higgs vev. While the couplings to W, Z, b, τ particles are derived by considering the decays of the Higgs boson to these particles, the $Ht\bar{t}$ coupling is derived indirectly from $\sigma(gg \rightarrow H)$ and $\text{BR}(H \rightarrow \gamma\gamma)$, two processes that are generated by triangular loops involving the top quarks in the SM. One can assume, in a first approximation, that $c_c = c_t$ and $c_\tau = c_b$ and possible invisible Higgs decays are absent. In Ref. [24], a three-dimensional fit of the H couplings was performed in the space $[c_t, c_b, c_V]$, when the theory uncertainty is taken as a bias and not as a nuisance. The results of this fit are presented in Fig. 3 (left) for $c_t, c_b, c_V \geq 0$. The best-fit value for the couplings, with the $\sqrt{s} = 7+8$ TeV ATLAS and CMS data turns out to be $c_t = 0.89$, $c_b = 1.01$ and $c_V = 1.02$, ie very close to the SM values.

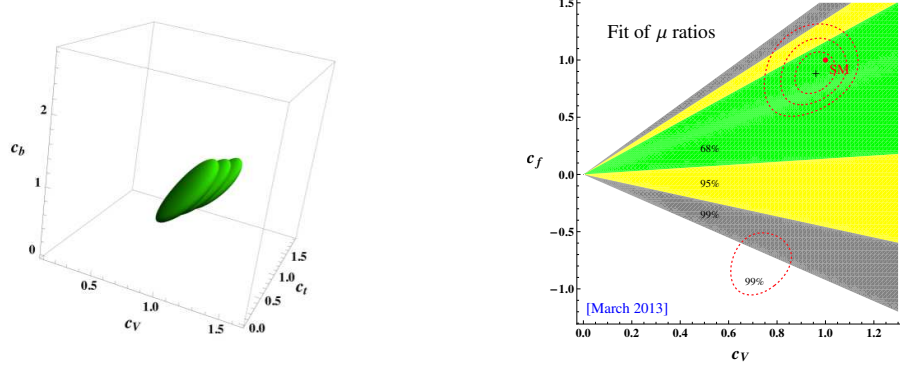


Figure 3: Left: the best-fit region at 68%CL for the Higgs signal strengths in the $[c_t, c_b, c_V]$ space [24]; the three overlapping regions are for the central and extreme choices of the theoretical prediction for the Higgs rates including uncertainties. Right: best-fit regions at 68%CL (green), 95%CL (yellow) and 99%CL (grey) in the plane c_f versus c_V ; the associated best-fit point (cross) and SM (red) point are also shown [23].

In the right-hand side of Fig. 3, a universal Higgs coupling to fermions $c_t = c_b = c_f$ is assumed and shown are the results when fitting the signal strengths as well as the Higgs decay branching ratios in the various modes. One sees that the best-fit domains from the ratios obtained e.g. at 1σ do not exclude parts of the 1σ regions obtained from the χ^2 since the main theoretical uncertainty cancels out in the D_{XX} ratios and is negligible for the signal strengths when added in quadrature to the experimental error. The domains from the likelihood fit are more restricted as the fit exploits the full experimental information on the Higgs rates and not only on the ratios and also, as the experimental error on a ratio of rates is higher than on the rates alone. The situation might improve in the future when the experimental uncertainty will decrease.

2.3 Implications of the Higgs couplings measurement

a) A fourth generation fermions?

One of the immediate implications of the LHC Higgs results is that a fourth generation of fermions (with a heavy neutrino $m_{\nu'} \gtrsim \frac{1}{2}M_Z$ to evade le LEP bounds [4]) is now completely ruled out [25]. Indeed, in addition to the direct LHC searches that exclude heavier quarks $m_{b'}, m_{t'} \lesssim 600$ GeV [26], strong constraints can be also obtained from the loop induced Higgs–gluon and Higgs–photon vertices in which any heavy particle coupling to the Higgs proportionally to its mass will contribute. In particular, for the $gg \rightarrow H$ leading process, the additional 4th generation t' and b' contributions increase the rate by a factor of ≈ 9 at LO. However, there are large $\mathcal{O}(G_F m_{f'}^2)$ electroweak corrections that affect these vertices, leading to a strong suppression of the $gg \rightarrow H \rightarrow \gamma\gamma$ rate, making this channel unobservable with four generations. Using a version of HDECAY with a fourth generation, one can show that the rate $\sigma(gg \rightarrow H) \times \text{BR}(H \rightarrow \gamma\gamma)|_{\text{SM4/SM}}$ for $M_H = 125$ GeV is a factor of 5 to 10 smaller than in the SM. Also, the ratio $\sigma(q\bar{q} \rightarrow VH) \times \text{BR}(H \rightarrow b\bar{b})|_{\text{SM4/SM}}$ is reduced by a factor 3 to 5 depending on $m_{\nu'}$. Hence with a fourth family, the Higgs signal would have not been observable and the obtained Higgs results unambiguously rule out this possibility.

b) Total width and invisible Higgs decays

Invisible decays would affect the properties of the observed Higgs particle and could be constrained if the total decay width is determined. But for a 125 GeV Higgs particle, $\Gamma_H^{\text{tot}} = 4$ MeV, is too small to be resolved experimentally. Nevertheless, in $pp \rightarrow VV \rightarrow 4f$, a large fraction of the Higgs cross section lies in the high–mass tail [27]. This allows to constrain Γ_H^{tot} and recent measurements of the ATLAS and CMS collaborations lead to a bound $\Gamma_H^{\text{tot}}/\Gamma_H^{\text{SM}} \approx 5\text{--}10$ [7]. These bounds are thus too loose and in addition strongly rely on the assumption that the off–shell Higgs couplings are exactly the same as the on–shell couplings, which is not true in many cases.

Nevertheless, the invisible Higgs decay width can be constrained indirectly by a fit of the Higgs couplings and in particular with the signal strength in the $H \rightarrow ZZ$ process: $\mu_{ZZ} \propto \Gamma(H \rightarrow ZZ)/\Gamma_H^{\text{tot}}$ with $\Gamma_H^{\text{tot}} = \Gamma_H^{\text{inv}} + \Gamma_H^{\text{SM}}$ and Γ_H^{SM} calculated with free coefficients c_f and c_V . The measurements give $\Gamma_H^{\text{inv}}/\Gamma_H^{\text{SM}} \lesssim 50\%$ at the 95% CL if the assumption $c_f = c_V = 1$ is made [23].

A more model independent approach would be to perform direct searches for missing transverse energy. These have been conducted by ATLAS and CMS in the $pp \rightarrow HV$ process with $V \rightarrow jj, \ell\ell$ and in the VBF channel, $qq \rightarrow qqE_T$. For $M_H \approx 125$ GeV a bound $\text{BR}_{\text{inv}} \lesssim 50\%$ is obtained at the 95%CL if the Higgs couplings are SM–like [7]. A more promising search for invisible decays is the monojet channel $gg \rightarrow Hj$ which has large rates [28]. Hence, if the Higgs is coupled to invisible particles, it may recoil against hard QCD radiation, leading to monojets. While the most recent monojet ATLAS and CMS searches [7] are only sensitive to an invisible rate close to unity, more restrictive results can be obtained with more data at the upgraded LHC.

The Higgs invisible rate and the dark matter detection rate in direct astrophysical searches are correlated in Higgs portal models. Considering the generic cases of scalar, fermionic and vectorial dark matter particles χ that couple only to the Higgs, one can translate in each case the LHC constraint $\text{BR}(H \rightarrow \text{inv.})$ into a constraint on the Higgs couplings to the χ particles. It turns out that these constraints are competitive [29] with those derived from the bounds on the dark matter scattering cross section on nucleons [30] from experiments such XENON for instance.

c) Determination of the spin–parity quantum numbers

Apart from the measurement of the couplings, one also needs to establish that the observed Higgs state is indeed a CP even scalar and hence with $J^{\text{PC}} = 0^{++}$ quantum numbers. For the spin, the observation of the $h \rightarrow \gamma\gamma$ decay rules out the spin-1 case by virtue of the Landau–Yang theorem [31]. The Higgs parity can be probed by studying kinematical distributions in the $H \rightarrow ZZ^* \rightarrow 4\ell$ decay channel and in the VH and VBF production modes [32].

With the 25 fb^{-1} data collected so far, the ATLAS and CMS collaborations performed a matrix-element likelihood analysis which exploits the kinematics and Lorenz structure of the $H \rightarrow ZZ^* \rightarrow 4\ell$ channel. It was found that the observed particle is more compatible with a 0^+ state and the 0^- possibility is excluded at the 97.8%CL or higher, as is shown in Fig. 4 (left) [33].

Other useful diagnostics of the Higgs CP nature that also rely on the tensorial structure of the HVV coupling can be made in the VBF process. It was known since a long time that in this channel, the distribution in the azimuthal angle between the two jets produced in association with the Higgs discriminates a CP-even from a CP-odd state [34]. This has been extended recently to other observables, like the rapidity separation between the two jets [35]. An example of discrimination between CP-even and CP-odd Higgs couplings (and also spin 2) is shown in Fig. 4 (center).

Nevertheless, there is a caveat in the analyses relying on the HVV couplings: since a CP-odd state has no tree-level VV couplings, the previous processes project out only the CP-even component of the HVV coupling [36] even if the state is a CP-even and odd mixture. Thus, in the CP studies above, one is simply verifying a posteriori that indeed the CP-even component is projected out. In fact, a better way to measure the Higgs parity is to study the signal strength in the $H \rightarrow VV$ channels [23]. Indeed, the HVV coupling takes the general form $g_{HVV}^{\mu\nu} = -ic_V(M_V^2/v) g^{\mu\nu}$ where c_V measures the departure from the SM: $c_V = 1$ for a pure 0^+ state with SM-like couplings and $c_V \approx 0$ for a pure 0^- state. The measurement of c_V should allow to determine the CP composition of the Higgs and in all cases, the quantity $1 - c_V^2$ gives an *upper bound* on the CP-odd contribution to the HVV coupling. Using μ_{VV} and the ratios $\mu_{\gamma\gamma}/\mu_{VV}$ and $\mu_{\tau\tau}/\mu_{VV}$, it was demonstrated that the observed Higgs has indeed a large CP component, $\gtrsim 50\%$ at the 95%CL; see Fig. 4 (right) [23].

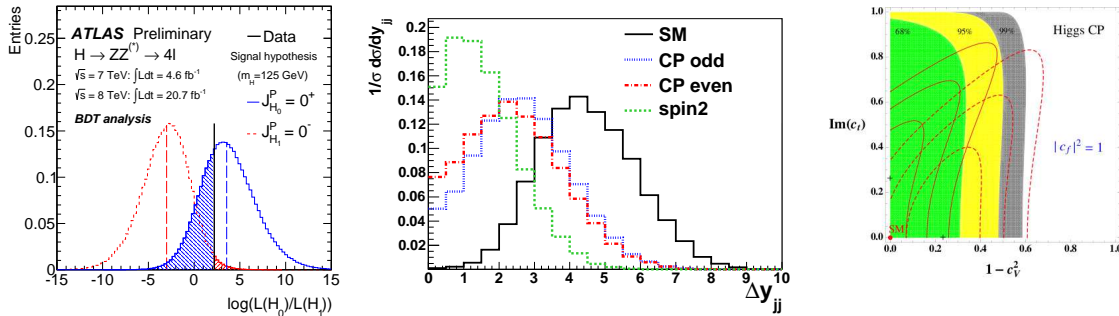


Figure 4: Left: discrimination between the 0^+ and 0^- Higgs hypotheses using the kinematics of the $H \rightarrow ZZ^* \rightarrow 4\ell$ channel by ATLAS [33]. Center: normalized distribution of the difference in rapidity between the scattered jets in VBF for each of the SM and BSM operators (spin-2, CP-even and CP-odd) individually [35]. Right: best-fit regions at 68%, 95% and 99%CL in the plane $[1 - c_V^2, \text{Im}(c_t)]$ for $|c_t|^2 = |c_f|^2 = 1$ [23].

In fact, it turns out that the best and less unambiguous way to probe the CP nature of the Higgs boson would be to look at final states in which the particle decays hadronically. The best examples would be then to consider the processes $pp \rightarrow HZ \rightarrow b\bar{b}l\ell$ and $pp \rightarrow t\bar{t}H \rightarrow t\bar{t}b\bar{b}$ and look for angular correlations [36]. These processes are nevertheless extremely challenging.

3. Implications for Supersymmetry

We turn now to the implications of the LHC Higgs results for the MSSM Higgs sector, first from the mass value and the production rates and then from heavy Higgs searches. We start by discussing the Higgs masses and couplings when the important radiative corrections are included.

3.1 The Higgs masses and couplings in the MSSM

In the MSSM, the tree-level masses of the CP-even h and H bosons depend only on M_A and $\tan\beta$. However, many parameters of the MSSM such as the masses of the third generation stop and sbottom squarks $m_{\tilde{t}}, m_{\tilde{b}_i}$ and their trilinear couplings A_t, A_b enter M_h and M_H through quantum corrections. These are introduced by a general 2×2 matrix $\Delta\mathcal{M}_{ij}^2$ but the by far leading is controlled by the top Yukawa coupling which appears with the fourth power in the 22 entry [14]

$$\Delta\mathcal{M}_{22}^2 \sim \frac{3\tilde{m}_t^4}{2\pi^2 v^2 \sin^2\beta} \left[\log \frac{M_S^2}{\tilde{m}_t^2} + \frac{X_t^2}{M_S^2} \left(1 - \frac{X_t^2}{12M_S^2} \right) \right], \quad \lambda_t = m_t/v \sin\beta \quad (3.1)$$

where $M_S = \sqrt{m_{\tilde{t}_1} m_{\tilde{t}_2}}$ is defined to be the SUSY-breaking scale and $X_t = A_t - \mu/\tan\beta$ the stop mixing parameter. Other soft SUSY-breaking parameters enter but their contribution is small. The maximal value M_h^{\max} is given in this approximation by $M_h^2 \xrightarrow{M_A \gg M_Z} M_Z^2 \cos^2 2\beta + \Delta\mathcal{M}_{22}^2$ and is obtained for: *i*) a decoupling regime $M_A \sim \mathcal{O}(\text{TeV})$; *ii*) large $\tan\beta$ values; *iii*) heavy stops, i.e. large M_S ; *iv*) the so-called maximal mixing scenario $X_t = \sqrt{6}M_S$ [37]. If the parameters are optimized as above, the maximal M_h value can reach the level of 130 GeV.

It was pointed out in Refs. [24, 38, 39] that when the measured value $M_h = 125$ GeV is taken into account, the MSSM Higgs sector with only the largely dominant $\Delta\mathcal{M}_{22}^2$ correction, can be again described with only the two parameters $\tan\beta$ and M_A ; in other words, the loop corrections are fixed by the value of M_h . This observation leads to a rather simple parametrisation of the MSSM Higgs sector, called h MSSM. One has for the heavier CP Higgs mass and the mixing angle α

$$M_H^2 = \frac{(M_A^2 + M_Z^2 - M_h^2)(M_Z^2 c_\beta^2 + M_A^2 s_\beta^2) - M_A^2 M_Z^2 c_{2\beta}^2}{M_Z^2 c_\beta^2 + M_A^2 s_\beta^2 - M_h^2}, \quad \alpha = -\arctan \left(\frac{(M_Z^2 + M_A^2) c_\beta s_\beta}{M_Z^2 c_\beta^2 + M_A^2 s_\beta^2 - M_h^2} \right) \quad (3.2)$$

while the charged Higgs mass is approximately given by its tree-level value $M_{H^\pm} \simeq \sqrt{M_A^2 + M_W^2}$. In Ref. [24], it has been shown that this h MSSM parametrisation is a very good approximation.

In the MSSM, the couplings of the CP-even h and H bosons compared to the SM Higgs couplings depend on the angles β and α . In the case of h outside the decoupling regime (where they reach unity), the reduced couplings to the heavy t, b, τ fermions and $V = W/Z$ bosons read

$$c_V^0 = \sin(\beta - \alpha), \quad c_t^0 = \cos\alpha/\sin\beta, \quad c_b^0 = -\sin\alpha/\cos\beta \quad (3.3)$$

If α is fixed by the h MSSM relation eq. (3.2), then the h couplings depend only on the inputs $\tan\beta, M_A$ as at tree-level. This is also the case of the heavier CP-even H boson. However, close to the decoupling regime that is indicated by the h properties, H has approximately the same mass as the A state and its interactions are similar. The MSSM Higgs spectrum will thus consist of a SM-like Higgs $h \equiv H_{\text{SM}}$ and two pseudoscalar-like particles, $\Phi = H/A$. The H^\pm boson will also be mass degenerate with the Φ states and the intensity of its couplings to fermions will be similar. In the high $\tan\beta$ regime, the couplings of the heavy Higgs bosons to b quarks and to τ leptons $\propto \tan\beta$ are so strongly enhanced, and the couplings to top quarks and W/Z bosons $\propto 1/\tan\beta$ suppressed, that the pattern is rather simple. At very low $\tan\beta$, the situation for the couplings is reversed.

3.2 Implications from the Higgs mass value

We discuss now the implications of the measured mass value of the observed Higgs boson at the LHC, that we identify with the lightest state h of the MSSM, relying mostly on Refs. [40, 41]. We will consider various options of the MSSM and Fig. 5 below summarises the findings.

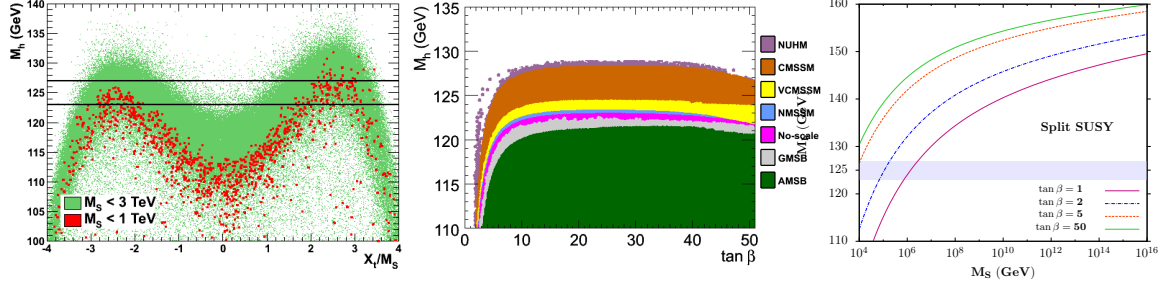


Figure 5: The maximal value of M_h in the MSSM [40]. Left: as a function of X_t/M_S in the pMSSM when all other SUSY parameters and $\tan\beta$ are scanned. Center: as function of $\tan\beta$ in various constrained MSSM scenarios. Right: as a function of M_S in split SUSY scenarios.

a) The phenomenological MSSM. In the so-called phenomenological MSSM (pMSSM) [42], in which CP conservation, flavour diagonal sfermion mass and coupling matrices and universality of the first and second sfermion generations are imposed, the model involves only 22 free parameters in addition to those of the SM: besides $\tan\beta$ and M_A , these are the higgsino mass μ , the three gaugino masses $M_{1,2,3}$, the diagonal left- and right-handed sfermion mass parameters $m_{\tilde{f}_{L,R}}$ and the trilinear sfermion couplings A_f . One can then perform a scan of these parameters in a wide range to obtain the maximal M_h^{\max} value with the full radiative corrections included.

Using the RGE program *Suspect* [43] that calculates the particle spectrum in the MSSM, a large scan of the pMSSM parameters was performed [40] and an illustration of the results is shown in Fig. 5 (left) where the obtained M_h^{\max} is displayed as a function of the ratio X_t/M_S . The resulting values are confronted to the mass range $123 \text{ GeV} \leq M_h \leq 127 \text{ GeV}$ when the $\pm 2 \text{ GeV}$ parametric uncertainties from the SM inputs and the theoretical uncertainties in the determination of M_h are included. For $M_S \lesssim 1 \text{ TeV}$, only the scenarios with X_t/M_S values close to maximal mixing $X_t/M_S \approx \sqrt{6}$ survive. The no-mixing scenario $X_t \approx 0$ is ruled out for $M_S \lesssim 3 \text{ TeV}$, while the typical mixing scenario, $X_t \approx M_S$, needs large M_S and moderate to large $\tan\beta$ values.

Note that masses above 1 TeV for squarks and gluinos are also required by the direct searches of SUSY particles at the LHC [44] confirming the need of high M_S values. Nevertheless, relatively light stops are still possible: as $M_S = \sqrt{m_{\tilde{t}_1} m_{\tilde{t}_2}}$, the possibility that $m_{\tilde{t}_1}$ is of the order of a few 100 GeV is still allowed, provided that stop mixing (leading to a significant $m_{\tilde{t}_1}, m_{\tilde{t}_2}$ splitting) is large. Light electroweak particles such as sleptons, charginos and neutralinos are also still possible allowing for a “natural SUSY” scenario [12] despite of the large value $M_h \approx 125 \text{ GeV}$.

b) Constrained MSSM scenarios. In constrained scenarios (cMSSM), the various soft SUSY-breaking parameters are a result of the RGE evolution and obey universal boundary conditions at a high scale, thus reducing the number of basic input parameters to a handful. Three classes of such models have been widely discussed [11]: the minimal supergravity (mSUGRA) model in which SUSY-breaking occurs in a hidden sector which communicates with the visible sector only via flavour-blind gravitational interactions leading to common $m_{1/2}, m_0, A_0$ values for the gaug-

ino masses, sfermion masses and sfermion trilinear couplings. Then come the gauge mediated and anomaly mediated SUSY-breaking scenarios, GMSB and AMSB, in which SUSY-breaking is communicated to the visible sector via gauge interactions and a super-Weyl anomaly. These models are described by $\tan\beta$, the sign of μ and a few continuous parameters.

Again, a large scan of these input parameters has been performed in Ref. [40, 41] with the constraint that $M_S \lesssim 3$ TeV not to allow for too much fine-tuning [12], and the results are shown in Fig. 5 (center) for several cMSSMs as a function of $\tan\beta$, the input that is common to all models. The resulting M_h^{\max} is 121 GeV in AMSB and 122 GeV in GMSB, which means that these two scenarios are disfavoured if $M_S \lesssim 3$ TeV. In mSUGRA, one obtains $M_h^{\max} = 128$ GeV and, thus, some parameter space would still survive; but in more constrained versions, the limit is lower. These limits can be qualitatively understood by considering the allowed values of the stop coupling A_t which in many cases cannot be large compared to M_S and hence does not allow maximal mixing.

c) Split and high-scale SUSY models. The choice $M_S \lesssim 3$ TeV made in the previous discussion is mainly dictated by fine-tuning considerations which are rather subjective. One could well abandon the SUSY solution to the hierarchy problem and have a very high M_S implying that, except for the h boson, all other scalar particles are inaccessible. This is the split SUSY scenario in which the soft SUSY-breaking scalar mass terms except for one Higgs doublet are assumed to have a common value $M_S \gg 1$ TeV. If the mass parameters for the spin- $\frac{1}{2}$ gauginos and higgsinos are also assumed to be large, we are then in a high scale SUSY scenario. See Ref. [45] for reviews.

In the Higgs sector, the main feature of these scenarios is that at the scale M_S , the boundary condition on the quartic Higgs coupling is determined by SUSY, $\lambda(M_S) = \frac{1}{4}[g^2(M_S) + g'^2(M_S)] \cos^2 2\beta$. But if the scalars are heavy, they lead to radiative corrections that are significantly enhanced by large $\log(M_S/M_Z)$ terms. In order to have reliable predictions, one needs to properly decouple the heavy states from the low-energy theory and resum the large logarithms. This work has been done in e.g. Ref. [46] and the results are implemented in the code `SuSpect` [43].

Using this tool, a scan in the $[\tan\beta, M_S]$ plane has been performed to determine the value of M_h in the split and high-scale SUSY scenarios. The requirement that $123 \lesssim M_h \lesssim 127$ GeV imposes strong constraints on the parameters of these two models. For this mass range and $\tan\beta \approx 1$, very large scales are needed in the high-scale SUSY scenario, while scales $M_S \approx 10^4$ GeV are required in the split-SUSY case; see Fig. 5 (right). In the latter case, to cope with $M_h = 125$ GeV, SUSY should manifest itself at much smaller scales at $\tan\beta \gg 1$, $M_S \approx 1$ TeV as seen previously.

d) Splitting the Higgs and sfermion sectors. In these high SUSY scale scenarios, the Higgs mass parameters were assumed to be related to the mass scale of the scalar fermions in such a way that the masses of the heavier Higgs particles are also large, $M_A \approx M_S$. However, this needs not to be true in general and one may be rather conservative and allow any value for M_A irrespective of M_S . This is the quite “model-independent” approach that has been advocated in Refs. [24, 38, 39]: take M_A as a free parameter of the pMSSM, with values ranging from $\mathcal{O}(100$ GeV) up to $\mathcal{O}(M_S)$.

An important consequence of this possibility is that it reopens the low $\tan\beta$ region, $\tan\beta \lesssim 3$, that was long thought to be forbidden if one requires a SUSY scale $M_S \lesssim 1$ TeV [37], as a result of the LEP2 limit $M_h \gtrsim 114$ GeV [4]. Values $\tan\beta \approx 1$ with a correct M_h are possible provided M_S is large enough, e.g. $M_S \approx 20$ TeV for $\tan\beta \approx 2$. In this scenario, one can use the h MSSM discussed in the previous subsection in which the Higgs sector with $M_h = 125$ GeV is again described by M_A and $\tan\beta$ at higher orders, which makes the discussion rather simple and transparent.

3.3 Implications from the production rates of the observed Higgs state

In the MSSM, the couplings of the Higgs particles depend in principle only on the two inputs $[\tan\beta, M_A]$ as discussed previously. However, this is true when only the radiative corrections to the Higgs masses and to the angle α are included. There are also direct corrections to the couplings which alter this simple picture and there are two important ones. First, for b -quarks, additional one-loop vertex corrections modify the tree-level Higgs- $b\bar{b}$ coupling: they grow as $m_b\mu\tan\beta$ and can be very large at high $\tan\beta$. These are the famous Δ_b corrections [47] which, outside the decoupling regime, make that the coupling $g_{hb\bar{b}} \propto c_b$ reads

$$c_b \approx c_b^0 \times [1 - \Delta_b/(1 + \Delta_b) \times (1 + \cot\alpha \cot\beta)] \quad (3.4)$$

with $\tan\alpha \rightarrow -1/\tan\beta$ for $M_A \gg M_Z$. A large Δ_b would significantly alter the dominant $h \rightarrow b\bar{b}$ partial width and affect the branching fractions of all other decays.

Second, the $ht\bar{t}$ coupling is derived indirectly from the $gg \rightarrow h$ production cross section and the $h \rightarrow \gamma\gamma$ decay branching ratio, two processes that are generated by triangular loops. In the MSSM, these loops involve not only the top quark (and the W boson in the decay $h \rightarrow \gamma\gamma$) but also contributions from not too heavy superparticles. In particular, there are stop loops that alter significantly the two process and change the coupling c_t^0 to [48]

$$c_t \approx c_t^0 [1 + m_t^2 / (4m_{t_1}^2 m_{t_2}^2) \times (m_{t_1}^2 + m_{t_2}^2 - X_t^2)] \quad (3.5)$$

Hence, because of these corrections, the Higgs should be characterized at the LHC by at least the three independent h couplings c_t , c_b and $c_V = c_V^0$ as discussed in section 2.2. The previously discussed fit, which allows to derive best-fit values $c_t = 0.89$, $c_b = 1.01$ and $c_V = 1.02$ of Fig. 6 can be used to constrain these corrections. In turn, ignoring the direct corrections (which are small for a high enough M_S) and using the input $M_h \approx 125$ GeV, one can make a fit in the plane $[\tan\beta, M_A]$. This is shown in the left-hand side of Fig. 6 where the 68%, 95% and 99% CL contours from the signal strengths and their ratios are displayed when the theory uncertainty is taken as a bias. The best-fit point is obtained $\tan\beta = 1$ and $M_A = 550$ GeV (which implies a large SUSY scale, $M_S = \mathcal{O}(100)$ TeV). Larger values of $\tan\beta$ and lower values of M_A could also be accommodated reasonably well by the fit, allowing thus for not too large M_S . In all, cases one has $M_A \gtrsim 200\text{--}350$ GeV though.

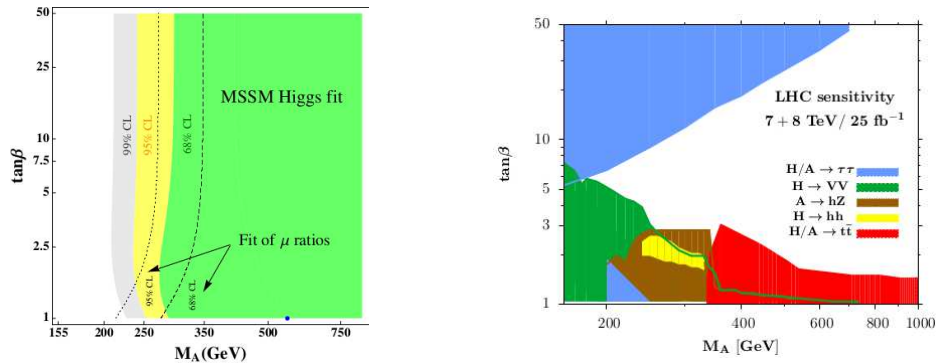


Figure 6: Left: best-fit regions for the signal strengths and their ratios in the plane $[\tan\beta, M_A]$; the best point is in blue [24]. Right: the estimated sensitivities in the various search channels for the heavier MSSM Higgs bosons in the $[\tan\beta, M_A]$ plane with the 25 fb^{-1} data collected so far at the 7+8 TeV LHC [38].

3.4 Implications from heavy Higgs boson searches

We turn now to the constraints on the MSSM Higgs sector that can be obtained from the search of the heavier H/A and H^\pm states at the LHC. At high $\tan\beta$ values, the strong enhancement of the b, τ couplings makes that the $\Phi = H/A$ states decay dominantly into $\tau^+\tau^-$ and $b\bar{b}$ pairs, with branching ratios of $\text{BR}(\Phi \rightarrow \tau\tau) \approx 10\%$ and $\text{BR}(\Phi \rightarrow b\bar{b}) \approx 90\%$, while the decays $\Phi \rightarrow t\bar{t}$ are negligible. The H^\pm boson decays into $\tau\nu_\tau$ final states with a branching fraction of almost 100% for H^\pm masses below the tb threshold, $M_{H^\pm} \lesssim m_t + m_b$, and a branching ratio of only $\approx 10\%$ for masses above this threshold while the rate for $H^\pm \rightarrow tb$ will be at the $\approx 90\%$ level in most cases. Concerning the production, only two processes are relevant in this case: $gg \rightarrow \Phi$ fusion with the b -loop included [49] and associated production with b -quarks, $gg/q\bar{q} \rightarrow b\bar{b} + \Phi$ [50]. The most powerful LHC search channel is thus $pp \rightarrow gg + b\bar{b} \rightarrow \Phi \rightarrow \tau^+\tau^-$. For the charged Higgs, the dominant mode is $H^\pm \rightarrow \tau\nu$ with the H^\pm light enough to be produced in top decays $t \rightarrow H^\pm b \rightarrow \tau\nu b$.

In the low $\tan\beta$ regime, $\tan\beta \lesssim 3$, the phenomenology of the A, H, H^\pm states is richer [38]. Starting with the production, there is no Higgs strahlung and VBF processes in the decoupling limit while the rates for associated $t\bar{t}\Phi$ and $b\bar{b}\Phi$ are small because the Φtt (Φbb) couplings are suppressed (not sufficiently enhanced). Only the $gg \rightarrow \Phi$ process with the dominant t and subdominant b contributions included provides large rates. For H^\pm , the dominant production channel is again top quark decays, $t \rightarrow H^\pm b$ for $M_{H^\pm} \lesssim 170$ GeV; for higher H^\pm masses, the main process is $gg/q\bar{q} \rightarrow H^\pm tb$. Turning to the $H/A/H^\pm$ decay pattern, it can be rather involved for $\tan\beta \lesssim 3$. Above the $t\bar{t}$ (tb) threshold for $H/A(H^\pm)$, the channels $H/A \rightarrow t\bar{t}$ ($H^+ \rightarrow t\bar{b}$) are by far dominant for and do not leave space for any other mode. Below the $t\bar{t}$ threshold, the $H \rightarrow WW, ZZ$ decay rates are still significant as g_{HVV} is not completely suppressed. For $2M_h \lesssim M_H \lesssim 2m_t$, $H \rightarrow hh$ is the dominant H decay mode as the Hhh self-coupling is large at low $\tan\beta$. For $M_A \gtrsim M_h + M_Z$, $A \rightarrow hZ$ decays would occur but the $A \rightarrow \tau\tau$ channel is still important with rates $\gtrsim 5\%$. In the case of H^\pm , the channel $H^\pm \rightarrow Wh$ is important for $M_{H^\pm} \lesssim 250$ GeV, similarly to the $A \rightarrow hZ$ case.

In Ref. [38] a preliminary analysis of these channels has been performed using current information given by the ATLAS and CMS collaborations in the context of searches for the SM Higgs boson or other heavy resonances. The results are shown in Fig. 6 (right) with an extrapolation to the full 25 fb^{-1} data of the 7+8 TeV LHC run (it has been assumed that the sensitivity scales simply as the square root of the number of events). The sensitivities from the usual $H/A \rightarrow \tau^+\tau^-$ and $t \rightarrow bH^\pm \rightarrow b\tau\nu$ channels directly taken from the ATLAS and CMS analyses [51] are also shown. The green and red areas correspond to the domains where the $H \rightarrow VV$ and $H/A \rightarrow t\bar{t}$ channels become constraining. The sensitivities in the $H \rightarrow hh$ and $A \rightarrow hZ$ modes are given by the yellow and brown areas which peak in the mass range $M_A = 250\text{--}350$ GeV at low $\tan\beta$ values.

The outcome of the searches is impressive. The ATLAS and CMS $H/A \rightarrow \tau^+\tau^-$ constraint is extremely restrictive and for $M_A \lesssim 250$ GeV, it excludes almost the entire intermediate and high $\tan\beta$ regimes. The constraint is less effective for a heavier A but even for $M_A \approx 400$ GeV the high $\tan\beta \gtrsim 10$ region is excluded and one is even sensitive to large values $M_A \approx 800$ GeV for $\tan\beta \gtrsim 50$. For the charged Higgs boson, almost the entire $M_{H^\pm} \lesssim 160$ GeV region is excluded by the process $t \rightarrow H^\pm b$ with the decay $H^\pm \rightarrow \tau\nu$. The other channels, in particular $H \rightarrow VV$ and $H/A \rightarrow t\bar{t}$, are very constraining as they cover the entire low $\tan\beta$ area that was previously excluded by the LEP2 bound up to $M_A \approx 500$ GeV. Even $A \rightarrow hZ$ and $H \rightarrow hh$ would be visible at the current LHC in small portions of the low $\tan\beta$ parameter space.

4. Perspectives for Higgs and new physics

The last few years were extremely rich and exciting for particle physics. With the historical discovery of a Higgs boson by the LHC collaborations ATLAS and CMS, crowned by a Nobel prize in fall 2013, and the first probe of its basic properties, they witnessed a giant step in the unraveling of the mechanism that breaks the electroweak symmetry and generates the fundamental particle masses. They promoted the SM as the appropriate theory, up to at least the Fermi energy scale, to describe three of Nature's interactions, the electromagnetic, weak and strong forces. However, it is clear that these few years have also led to some frustration as no signal of physics beyond the SM has emerged from the LHC data. The hope of observing some signs of the new physics models that were put forward to address the hierarchy problem, that is deeply rooted in the Higgs mechanism, with Supersymmetric theories being the most attractive ones, did not materialize.

The Higgs discovery and the non-observation of new particles has nevertheless far reaching consequences for supersymmetric theories and, in particular, for their simplest low energy formulation, the MSSM. The mass of approximately 125 GeV of the observed Higgs boson implies that the scale of SUSY-breaking is rather high, at least $\mathcal{O}(\text{TeV})$. This is backed up by the limits on the masses of strongly interacting SUSY particles set by the ATLAS and CMS searches, which in most cases exceed the TeV range. This implies that if SUSY is indeed behind the stabilization of the Higgs mass against very high scales that enter via quantum corrections, it is either fine-tuned at the permille level at least or its low energy manifestation is more complicated than expected.

The production and decay rates of the observed Higgs particles, as well as its spin and parity quantum numbers, as measured by ATLAS and CMS with the $\approx 25 \text{ fb}^{-1}$ data collected at $\sqrt{s}=7+8$ TeV, indicate that its couplings to fermions and gauge bosons are almost SM-like. In the context of the MSSM, this implies that we are close to the decoupling regime and this particle is the lightest h boson, while the other $H/A/H^\pm$ states must be heavier than approximately the Fermi scale. This last feature is also backed up by LHC direct searches of these heavier Higgs states.

This drives up to the question that is now very often asked: what to do next? The answer is, for me, obvious: we are only in the beginning of a new era. Indeed, it was expected since a long time that the probing of the electroweak symmetry breaking mechanism will be at least a two chapters story. The first one is the search and the observation of a Higgs-like particle that will confirm the scenario of the SM and most of its extensions, that is, a spontaneous symmetry breaking by a scalar field that develops a non-zero vev. This long chapter has just been closed by the ATLAS and CMS collaborations with the spectacular observation of a Higgs boson. This observation opens a second and equally important chapter: the precise determination of the Higgs profile and the unraveling of the electroweak symmetry breaking mechanism itself.

A more accurate measurement of the Higgs couplings to fermions and gauge bosons will be mandatory to establish the exact nature of the mechanism and, eventually, to pin down effects of new physics if additional ingredients beyond those of the SM are involved. This is particularly true in weakly interacting theories such as SUSY in which the quantum effects are expected to be small. These measurements could be performed at the upgraded LHC with an energy close to $\sqrt{s}=14$ TeV, in particular if a very high luminosity, a few ab^{-1} , is achieved [51, 52].

At this upgrade, besides improving the measurements performed so far, rare but important channels such as associated Higgs production with top quarks, $pp \rightarrow t\bar{t}H$, and Higgs decays into

$\mu^+\mu^-$ and $Z\gamma$ states could be probed. Above all, a determination of the self-Higgs coupling could be made by searching for double Higgs production e.g. in the gluon fusion channel $gg \rightarrow HH$ [53]; this would be a first step towards the reconstruction of the scalar potential that is responsible of electroweak symmetry breaking. This measurement would be difficult at the LHC even with high-luminosity but a proton collider with an energy $\sqrt{s}=30$ to 100 TeV could do the job [52].

In a less near future, a high-energy lepton collider, which is nowadays discussed in various options (ILC, TLEP, CLIC, μ -collider) would lead to a more accurate probing of the Higgs properties [54], promoting the scalar sector to the very high-precision level of the gauge and fermion sectors achieved by the LEP and SLC colliders in the 1990s [4]. In e^+e^- collisions, the process $ee \rightarrow HZ$, just looking at the recoiling Z boson allows to measure the Higgs mass, the CP parity and the absolute HZZ coupling, allowing to derive the total decay width Γ_H^{tot} . One can then measure precisely, already at $\sqrt{s} \approx 250$ GeV where $\sigma(e^+e^- \rightarrow HZ)$ is maximal, the absolute Higgs couplings to gauge bosons and light fermions at the % level from the decay branching ratios. The important couplings to top quarks and the Higgs self-couplings can be measured at the 10% level in the higher-order processes $e^+e^- \rightarrow t\bar{t}H$ and $e^+e^- \rightarrow HHZ$ at energies of at least 500 GeV with a high-luminosity. Some information on this issue is given in Fig. 7.

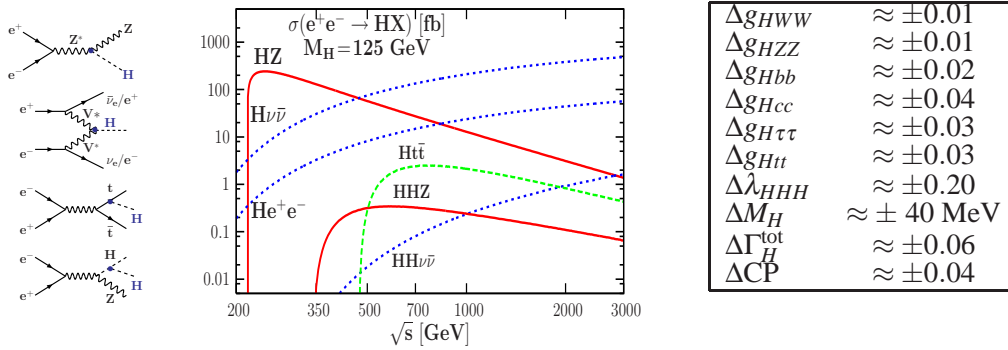


Figure 7: Diagrams for Higgs production in e^+e^- collisions (left), production cross sections for a 125 GeV SM-Higgs as a function of \sqrt{s} (center) and expected accuracies (right) for various coupling measurements (as well as mass, total width and CP-odd mixture) at the ILC with energy up to $\sqrt{s} = 500$ GeV and a luminosity of up to 500 fb^{-1} (see the discussion in G. Aarons et al. in Ref. [54]).

Besides the high precision study of the already observed Higgs, one should also continue to search for the heavy states that are predicted by SUSY, not only the superparticles but also the heavier Higgs bosons. The energy upgrade to ≈ 14 TeV (and eventually beyond) and the planned order of magnitude (or more) increase in luminosity will allow to probe much higher mass scales than presently. In fact, more generally, one should continue to search for any sign of new physics or new particles, new gauge bosons and fermions, as predicted in most of the SM extensions.

In conclusion, it is not yet time to give up on SUSY and more generally on new physics but, rather, to work harder to be fully prepared for the more precise and larger data set that will be delivered by the upgraded LHC. It will be soon enough to “philosophize” then as the physics landscape will become more clear.

Acknowledgements: I would like to thank the organisers for their invitation to the school and their kind hospitality. This work is supported by the ERC Advanced Grant Higgs@LHC.

References

- [1] ATLAS collaboration, Phys. Lett. B716 (2012) 1; CMS collaboration, Phys. Lett. B716 (2012) 30.
- [2] F. Englert and R. Brout, Phys. Rev. Lett. 13 (1964) 321; P. Higgs, Phys. Rev. Lett. 13 (1964) 508; P. Higgs, Phys. Lett. 12 (1964) 132; G. Guralnik, C. Hagen, T. Kibble, Phys. Rev. Lett. 13 (1964) 585.
- [3] For a review of Higgs physics in the SM, see: A. Djouadi, Phys. Rept. 457 (2008) 1.
- [4] K. Olive et al., Particle Data Group, Chin. Phys. C38 (2014) 090001.
- [5] B.W. Lee, C. Quigg and H.B. Thacker, Phys. Rev. D16 (1977) 1519.
- [6] N. Cabibbo et al., Nucl. Phys. B158 (1979) 295; M. Sher, Phys. Rept. 179 (1989) 273; T. Hambye and K. Riesselmann, Phys. Rev. D55 (1997) 7255; J. Ellis et al., Phys. Lett. B679 (2009) 369.
- [7] Updated analyses of the Higgs sector can be found in the slides of the talks given at the Moriond Electroweak conference, March 2015: <https://indico.in2p3.fr/event/10819/other-view?view=standard>.
- [8] G. Degrossi et al., JHEP 1208 (2012) 098; F. Bezrukov et al., JHEP 1210 (2012) 140.
- [9] S. Alekhin, A. Djouadi and S. Moch, Phys. Lett. B716 (2012) 214.
- [10] See the lectures of G. Altarelli, I. Antoniadis and D. Kazakov, these proceedings.
- [11] M. Drees, R. Godbole and P. Roy, *Theory and phenomenology of sparticles*, World Sci., 2005.
- [12] E. Witten, Nucl. Phys. B188 (1981) 513; Nucl. Phys. B202 (1982) 253; R. Barbieri and G. Giudice, Nucl. Phys. B306 (1988) 63; M. Papucci, J. Ruderman and A. Weiler, JHEP 1209 (2012) 035.
- [13] A. Djouadi, Phys. Rept. 459 (2008) 1; see also Eur. Phys. J. C74 (2014) 2704 for a recent update.
- [14] For reviews, see: S. Heinemeyer, W. Hollik and G. Weiglein, Phys. Rept. 425 (2006) 265; M. Carena and H. Haber, Prog. Part. Nucl. Phys. 50 (2003) 63; B. Allanach et al., JHEP 0409 (2004) 044.
- [15] A. Djouadi, J. Kalinowski and M. Spira, Comput. Phys. Commun. 108 (1998) 56; A. Djouadi, M. Muhlleitner and M. Spira, Acta. Phys. Polon. B38 (2007) 635.
- [16] H. Georgi et al., Phys. Rev. Lett. 40 (1978) 692; A. Djouadi, M. Spira and P.M. Zerwas, Phys. Lett. B264 (1991) 440; S. Dawson, Nucl. Phys. B359 (1991) 283; R. Harlander and W. Kilgore, Phys. Rev. Lett. 88 (2002) 201801; C. Anastasiou and K. Melnikov, Nucl. Phys. B646 (2002) 220; V. Ravindran, J. Smith and W.L. Van Neerven, Nucl. Phys. B665 (2003) 325; S. Catani et al, JHEP 0307 (2003) 028.
- [17] A. Djouadi and P. Gambino, Phys. Rev. Lett. 73 (1994) 2528; Nucl. Phys. B523 (1998) 17; G. Degrossi and F. Maltoni, Phys. Lett. B600 (2004) 255; S. Actis et al., Phys. Lett. B670 (2008) 12.
- [18] J. Baglio and A. Djouadi, JHEP 1103 (2011) 055; see also: JHEP 1010 (2010) 064; J. Baglio, A. Djouadi and R. Godbole, Phys. Lett. B716 (2012) 203.
- [19] S. Dittmaier et al., the LHC Higgs cross section working group, arXiv:1101.0593 [hep-ph].
- [20] A. Djouadi, Eur. Phys. J. C73 (2013) 2498.
- [21] S. Dittmaier et al., the LHC Higgs cross section working group: arXiv:1201.3084 [hep-ph].
- [22] D. Zeppenfeld, R. Kinnunen, A. Nikitenko and E. Richter-Was, Phys. Rev. D62 (2000) 013009; A. Djouadi et al., hep-ph/0002258; M. Dührssen et al., Phys. Rev. D70 (2004) 113009.
- [23] A. Djouadi and G. Moreau, Eur. Phys. J. C73 (2013) 2512.
- [24] A. Djouadi, L. Maiani, G. Moreau, A. Polosa, J. Quevillon, V. Riquer, Eur. Phys. J. C73 (2013) 2650; see also arXiv:1502.05653 [hep-ph] for an update.

- [25] A. Djouadi and A. Lenz, Phys. Lett. B715 (2012) 310; E. Kuflik, Y. Nir and T. Volansky, Phys. Rev.Lett. 110 (2013) 091801; A. Denner et al., Eur.Phys.J. C72 (2012) 1992.
- [26] CMS collab., Phys. Rev. D86 (2012) 112003; ATLAS collab., Phys. Rev. Lett. 109 (2012) 032001.
- [27] See e.g., N. Kauer and G. Passarino, JHEP 1208 (2012) 116.
- [28] A. Djouadi, A. Falkowski, Y. Mambrini and J. Quevillon, Eur. Phys. J. C73 (2013) 2455.
- [29] A. Djouadi, O. Lebedev, Y. Mambrini and J. Quevillon, Phys. Lett. B709 (2012) 65.
- [30] M. Goodman and E. Witten, Phys. Rev. D31 (1985) 3059; M. Drees and M. Nojiri, Phys.Rev. D47 (1993) 4226; Phys. Rev. D48 (1993) 3483; A. Djouadi and M. Drees, Phys. Lett. B484 (2000) 183.
- [31] L. Landau, Dokl. Akad. Nauk Ser. Fiz. 60 (1948) 207; C. Yang, Phys. Rev. 77 (1950) 242.
- [32] For a review of the CP Higgs issue, see e.g. S. Kraml (ed.) et al., hep-ph/0608079.
- [33] ATLAS collab., Phys. Lett. B726 (2013) 120; CMS collab., Phys. Rev. Lett. 110 (2013) 081803.
- [34] T. Plehn, D. Rainwater and D. Zeppenfeld, Phys. Rev. Lett. 88 (2002) 051801.
- [35] A. Djouadi, R. Godbole, B. Mellado, K. Mohan, Phys. Lett. B723 (2013) 307.
- [36] V. Barger et al., Phys. Rev. D49 (1994) 79; B. Grzadkowski, J. Gunion and X. He, Phys. Rev. Lett. 77 (1996) 5172; J. Gunion and J. Pliszka, Phys. Lett. B444 (1998) 136; P. Bhupal Dev et al., Phys. Rev. Lett. 100 (2008) 051801; J. Ellis, V. Sanz and T. You, Phys. Lett. B726 (2013) 244.
- [37] M. Carena et al., Eur. J. Phys. C26 (2003) 601; Eur. Phys. J. C73 (2013) 2552.
- [38] A. Djouadi and J. Quevillon, JHEP 1310 (2013) 028.
- [39] L. Maiani, A. Polosa and V. Riquer, Phys. Lett. B718 (2012) 465; Phys. Lett. B724 (2013) 274.
- [40] A. Arbey et al., Phys. Lett. B708 (2012) 162.
- [41] A. Arbey et al., JHEP 1209 (2012) 107; Phys. Lett. B720 (2013) 153.
- [42] A. Djouadi et al. (MSSM working group), hep-ph/9901246.
- [43] A. Djouadi, J.L. Kneur and G. Moultaka, Comput. Phys. Commun. 176 (2007) 426; M. Muhlleitner et al., Comput. Phys. Commun. 168 (2005) 46.
- [44] For a review of SUSY constraints at the LHC, see e.g. N. Craig, arXiv:1309.0528 [hep-ph].
- [45] L. Hall and Y. Nomura, JHEP 03 (2010) 076; G. Giudice and A. Strumia, Nucl. Phys. B858 (2012) 63.
- [46] N. Bernal, A. Djouadi, P. Slavich, JHEP 0707 (2007) 016.
- [47] See e.g., M. Carena et al., Nucl. Phys. B577 (2000) 88.
- [48] A. Djouadi et al., Phys. Lett. B435 (1998) 101; Eur. Phys. J.C1 (1998) 149; Eur. Phys. J.C1 (1998) 163; A. Arvanitaki, G. Villadoro, JHEP 02 (2012) 144; A. Delgado et al., Eur.Phys.J.C73 (2013) 2370;
- [49] M.Spira et al., Phys. Lett. B318 (1993) 347; Nucl. Phys. B453 (1995) 17.
- [50] R. Harlander and W. Kilgore, Phys. Rev. D68 (2003) 013001; R. Harlander, S. Liebler and H. Mantler, Comp. Phys. Comm. 184 (2013) 1605.
- [51] ATLAS collaboration, arXiv:1307.7292; CMS collaboration, arXiv:1307.7135.
- [52] S. Dawson et al., arXiv:1310.8361 [hep-ex].
- [53] See e.g., J. Baglio et al., JHEP 1304 (2013) 151.
- [54] M. Bicer et al., arXiv:1308.6176; H. Baer et al., arXiv:1306.6352; G. Arons et al., arXiv:0709.1893; J. Aguilar-Saavedra, hep-ph/0106315; E. Accomando et al., Phys. Rept. 299 (1998) 1; A. Djouadi, Int. J. Mod. Phys. A10 (1995) 1; Acta Phys.Polon.B37 (2006) 1367.